Chapter 10

Growth and Development of Sapphire Crystal for LED Applications

Huili Tang, Hongjun Li and Jun Xu

Additional information is available at the end of the chapter

http://dx.doi.org/10.5772/54249

1. Introduction

LEDs (Light emitting diodes) are considered as the most promising green lighting sources in 21st Century for the advantages in high brightness, long lifetime (more than 50,000 hours), low energy consumption, short corresponding time, good shock resistance, non-toxic, recyclable, safety. LEDs have already been extensively used in outdoor displays, traffic lights, high-performance back light units in liquid-crystal displays, general lighting. Strategies Unlimited Company predicted that the compound annual growth rate (CAGR) of the LED market would increase to 30.6%, up to $20.2 billion in 2014. It is obvious that incandescent bulbs and fluorescent lamps will be replaced by LEDs, which could alleviate the increasingly serious global energy crisis. Therefore, the development of semiconductor lighting industry is of great significance. Many countries have already launched National Semiconductor Lighting Plan, investing heavily in researching and developing the LEDs industry. In 1998, Japan made a "Light for the 21st Century" plan with the budget of 6 billion yen. In July 2000, European Union implemented "Rainbow project bring color to LEDs" plan, setting up ECCR and promoting the application of white light LED through the EU BRITE/ EURAM-3 program. U.S. Department of Energy established "National research program on semiconductor lighting" plan. It is expected that in 2025, the use of solid state lighting will reduce half of the lighting electricity consumption and save $35 billion per year. In June 2003, the Chinese Ministry of Science and Technology launched an "National Semiconductor Lighting Project" in support of the "863" Project. In 2009, ministry of Science and Technology started "Ten thousand LED lights in ten cities" semiconductor lighting demonstration program. It is expected that in 2015, semiconductor lighting will occupy 30% of the domestic general lighting market.

The luminescent property of LED is being continuously improved under the research all over the world. In 2002, Lumileds Company made the LED with the luminous efficiency of 18-22 lm/W. In February 2009, Nichia Company fabricated a white LED with luminous efficiency of 249 lm/W under 20mA driving current. As a leading manufacturer in the field of LED, Cree Company has produced mass production products with the highest luminous efficiency of 161 lm/W in 2011. Later after that, in April 2012 they announced that the white power type LED with luminous efficiency up to 254 lm/W under 350mA driving current has been manufactured successfully, which again refreshed the industry record.

LED industry is divided into upstream, midstream and downstream chains. Upstream chain includes substrate material, epitaxial wafers and chip manufacturing; midstream chain includes packaging and devices; and various LED application products belong to downstream chain. As a cornerstone of the development of semiconductor lighting industry, to some extent, the development of substrate material determines the route of the development of semiconductor lighting technology. Therefore, substrate material is a critical core issue of current semiconductor lighting industry.

The main factors determining the appropriate substrate materials are matched lattice parameters and thermal expansion coefficients as well as good crystallinity, chemical, physical and mechanical properties. Many materials were investigated as substrates, such as sapphire (α-Al_2O_3), SiC, Si, GaAs, $MgAl_2O_4$, $ScAlMgO_4$, γ-$LiAlO_2$ and β-$LiGaO_2$ etc. Table 1 shows the related parameters of some substrate materials for GaN and ZnO epitaxy [1]. Among them, sapphire and SiC are the main commercial substrates. Due to SiC substrate is very expensive, sapphire is the most important semiconductor LED lighting industry substrate. According to a conservative estimation, the demand of epi-ready sapphire substrate in international market is 600,000 pieces per month. In order to reduce Metal-organic Chemical Vapor Deposition (MOCVD) epitaxial cost, the requirement of substrate wafer size is getting larger and larger, from 2″ to 4″, 6″ and 8″. Therefore, the growth and development of large size sapphire crystal have attracted increasing attention all over the world.

This chapter investigates the strengthening and toughening of sapphire crystal by ion doping. Besides, the chapter is devoted to review the raw material, seed crystal, growth direction and growth methods, which have influence on the quality of sapphire crystal. The latest progress in the main growth methods of sapphire substrate: Kyropoulos method, heat exchanger method, Czochralski method, edge-defined film-fed growth method and temperature gradient technique are systematical illustrated. Finally, the overall evaluation on the advantage and disadvantage of each method is briefly outlined.

2. Properties of sapphire crystal

2.1. Crystal structure

Sapphire crystal is a simple coordinated type oxide crystal, whose chemical constituent is Al_2O_3 and crystalline form is α-Al_2O_3. Sapphire, also named corumdum, belongs to trigonal

http://dx.doi.org/10.5772/54249

Substrate	Structure	Space group	Lattice constant (Å)	Thermal expansion ($\times 10^{-6}$ K^{-1})	Lattice mismatch	
					GaN	ZnO
w-GaN	wurtzite	$P6_3mc$	a=3.188 c=5.185	5.59 3.17	0%	-1.9%
ZnO	wurtzite	$P6_3mc$	a=3.250 c=5.206	2.9 4.75	1.9%	0%
α-Al_2O_3	rhombohedral	$R\bar{3}c$	a=4.757 c=12.983	7.5 8.5	-14%	18.4%
6H-SiC	6H (W)	$P6_3mc$	a=3.081 c=15.117	4.46 4.16	-3.3%	3.5%
Si	diamond	$Fd\bar{3}m$	a=5.430	3.59	20.4%	18.1%
GaAs	zincblende	$F\bar{4}3m$	a=5.6533	6.0	-20%	-19%
$MgAl_2O_4$	spinel	$Fd\bar{3}m$	a=8.083	7.45	-10.3%	-12.1%
$Mg_{0.4}Al_{2.4}O_4$	spinel	$Fd\bar{3}m$	a=7.984	5.62	-11.4%	-13.1%
$ScMgAlO_4$	tetragonal	$R\bar{3}m$	a=3.246 c=25.195	6.2 12.2	1.8%	0.09%
γ-$LiAlO_2$	tetragonal	$P4_12_12$	a=5.169 c=6.268	7.1 15	-1.7%	-3.5%
β-$LiGaO_2$	orthorhombic	$Pna2_1$	a=5.402 b=6.372 c=5.007	1.7 11.0 4.0	-0.2%	2%

Table 1. Related parameters of the substrate materials for GaN and ZnO epitaxy.

system, $D_{3d}^6 - R\bar{3}C$ space group. It has symmetry elements as follows: mirror-turn axis of the sixth order (ternary inversion axis), three axes of the second order normal to it, three symmetry planes normal to the axes of the second order and intercrossing along the axis of the highest order and symmetry center [2.3]. The crystal lattice of sapphire is formed by Al^{3+} and O^{2-} ions. The crystal lattice takes the form of O^{2-} ions closest hexagonal packing and Al^{3+} cations locate in the octahedral hollows between the closely packed O^{2-} ions, filling two thirds of these hollows (see Figure 1). Polarity, semi-polarity and non polarity GaN films can be grown on different orientation sapphire substrates. The epitaxial relationship of $(11\bar{2}2)$ semipolar GaN film on $(10\bar{1}0)$ m-plane sapphire substrate is $[10\bar{1}0]_{GaN} \| [1\bar{2}10]_{sapphire}$, $[1\bar{2}1\bar{1}]_{GaN} \| [0001]_{sapphire}$, and $(11\bar{2}0)$ nopolar GaN film on $(1\bar{1}02)$ r-plane sapphire substrate is $[1\bar{1}00]_{GaN} \| [11\bar{2}0]_{sapphire}$, $[0001]_{GaN} \| [\bar{1}101]_{sapphire}$ [5-7].

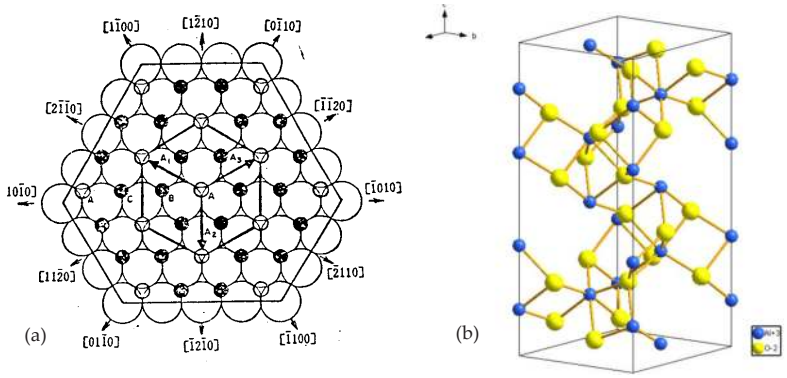

Figure 1. a) Schematic of the packing of O^{2-} ions in the sapphire cell,(b) Rhombodedral unite cell of the sapphire crystal.

2.2. Physical, thermal, optical and electrical properties

Sapphire is a high melting point oxide crystal (2050℃), which can be used at the highest temperature of 1900℃. Table 2 presents the main properties of the sapphire crystal. Sapphire has a high refractive index and a broad transmission band from 0.14 to 6.0 μm, spanning the UV, visible, and IR bands. Sapphire also has a high hardness (next to diamond) and surface smoothness, very good tensile strength, thermal conductivity, electric insulation, wear resistance, and thermal shock resistance [10-12]. The chemical properties of sapphire are very stable. Generally, sapphire is insoluble in water; insoluble in nitric acid (HNO_3), sulfuric acid (H_2SO_4), hydrochloric acid (HCL), hydrofluoric acid (HF) and phosphoric acid (H_3PO_4) up to 300°C; and insoluble in alkalis up to 800°C. The favorable combination of excellent optical and mechanical properties of sapphire, together with high chemical durability, makes it a desirable substrate material for LED applications.

Physical Properties	
Chemical Formula	Al_2O_3
Structure	hexagonal-rhombodedral
Molecular weight	101.96
Lattice Constants Å	a=4.765, c=13,000
Crystal density (g/cm^3)	3.98
Melt density (g/cm^3)	3.0
Hardness	9 Mohs 1800 knoop parallel to C-axis 2200 knoop perpendicular to C-axis

http://dx.doi.org/10.5772/54249

Young Modulus (GPa)	379 at 30° to C-axis 352 at 45° to C-axis 345 at 60° to C-axis 386 at 75° to C-axis
Shear Modulus (GPa)	145
Bulk Modulus (GPa)	240
Bending Modulus/ Modulus of Rupture (MPa)	350 to 690
Tensile strength	400 at 25°C 275 at 500°C 345 at 1000°C
Elastic Coefficient	C=496, C12=164, C13=115, C33=498, C44=148
Apparent Elastic Limit (MPa)	448 to 689
Flexural Strength (GPa)	2.5 - 4.0
Poisson ratio	0.25 - 0.30
Friction Coefficient	0.15 on steel 0.10 on sapphire
Abrasion resistance	8 times higher than steel
Thermal Properties	
Melting Point (°C)	2050
Specific Heat J/(kg ·K)	105 at 91 K 761 at 291 K
Thermal coefficient of linear expansion at 323 K (K^{-1})	66.66×10^{-6} parallel to optical axis 5×10^{-6} perpendicular to optical axis
Thermal conductivity (W/m °K) at 20°C	41.9
Thermal Expansion (20-1000°C)	Parallel to C-axis: 9.03×10^{-6} °C Perpendicular to C-axis: 8.31×10^{-6} °C 60° to C-axis: 8.4×10^{-6} °C
Optical Properties	
Transission Range	0.2 - 5.5 microns
Reflection loss	14% at 1 micron (2 surfaces)
Restrahlen Peak	13.5 micron
dN/dT	$+13\times10^{-6}$ °C
Refractive index	1.7122
T_t%	87.1

Electrical Properties	
Resistivity, Ohm•cm at 20 - 500°C	10^{11} - 10^{16}
Dielectric Constant	11.5 parallel to C axis 9.4 perpendicular to C axis
Dielectric strength (V/cm)	4×10^{5}
Loss Tangent	10^{-4}

Table 2. Main physical, thermal, optical and electrical properties of the sapphire crystal.

2.3. Improving mechanical properties of sapphire by ion doping

Because of excellent physical and chemical properties and outstanding spectrum transmission performance in wide bands range, sapphire crystal has been widely applied in various kinds of high-end window materials and LED substrates. But sapphire crystal is prone to brittle fracture at room temperature, causing the decline of mechanical properties and thermal shock resistance. So strengthening and toughening of sapphire at room temperature have important value on both scientific research and practical applications.

2.3.1. Strengthen and toughen sapphire by carbon doping

Figure 2 shows the carbon-doped sapphire (C:sapphire) single crystals grown by TGT method and the crystal was colored because of carbon doping. The C:sapphire crystal possessed remarkable absorption peaks at 206 nm and 256 nm (see Figure 3). The fracture strength and fracture toughness of C:sapphire and sapphire crystals along [$11\bar{2}0$] direction on (0001) plane are listed in Table 3. The fracture strength and fracture toughness of 1000 ppm C:sapphire crystal (No.2) were 752.0 MPa and 2.81 Mpa $m^{1/2}$, respectively. The fracture strength and fracture toughness of undoped sapphire crystals (No. 0) were 488.25 MPa and 1.99 Mpa $m^{1/2}$, respectively. It is demonstrated that the mechanical properties of sapphire crystal can be greatly improved by carbon doping.

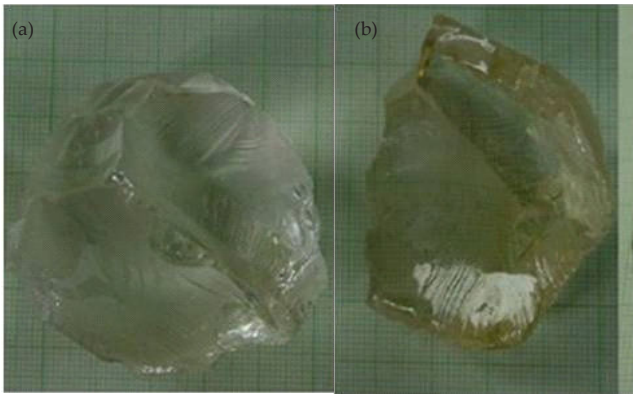

Figure 2. C:sapphire crystal grown by TGT method: (a) 2000 ppm C:sapphire, (b) 5000 ppm C:sapphire

http://dx.doi.org/10.5772/54249

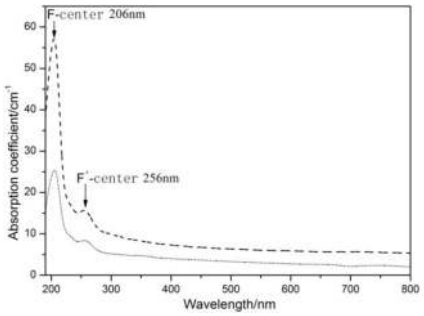

Figure 3. Absorption spectrum of C:sapphire.

Sample/Test	No.0	No.1	No.2
Fracture strength (MPa)	488.25	597.75	752.0
Fracture toughness(MPa·$m^{1/2}$)	1.99	2.41	2.81

Table 3. Mechanical properties of C:sapphire and sapphire crystals at room temperature

The doped carbon itself occurred disproportionating reaction at high temperature in the process of crystal growth, i.e. $3C \rightarrow 2C^{2+}+C^{4-}$. C^{4-} ions substituted negative oxygen ions (O^{2-}) and generated oxygen vacancy defects (Vo). Vo captured one or two electronic and formed F^{+} or F color centers. Consequently, the absorption peaks at 206 nm and 256 nm of C:sapphire were strengthened significantly. And the C^{2+} whose radius is only 0.16 Å entered the lattice in the form of interstitial ion, which created blocking effect to the sapphires cracking and improved fracture strength and fracture toughness of sapphire crystal at room temperature.

2.3.2. Strengthen and toughen sapphire by titanium doping

Figure 4(a) shows titanium doped sapphire single crystal grown by Vertical Bridgman Method and the crystal was colored because of Ti^{3+} doping. After annealing at 1600°C for 24h in the air atmosphere, the crystal was colorless and the absorption peak of Ti^{3+} ion significantly weakens in the absorption spectrum. Meanwhile, we found that the mechanical properties of sapphire can be improved through titanium doping, as is shown in Figure 5. At room temperature, the fracture strength and fracture toughness of Ti^{3+}: sapphire along $[11\bar{2}0]$ direction on (0001) plane were 560 MPa and 2.29 MPa $m^{1/2}$ respectively. And the fracture strength and fracture toughness of Ti^{4+}: sapphire single crystal (annealing from Ti^{3+}: sapphire under 1600°C for 24h) are 600 MPa and 2.35 MPa $m^{1/2}$ respectively. It has been found that Ti^{3+} and Ti^{4+} doping was beneficial to improve mechanical property of the sapphire crystal. Solid solution reaction of doped titanium ions occurred during crystal growth processes and the aluminum ions of the matrix were substituted by titanium ions. The solid solution

makes the fracture strength and fracture toughness of doped sapphire improved. After annealing at 1600°C for 24h, doped Ti^{3+} ions were oxidized to Ti^{4+} ions. While Al^{3+} was substituted by Ti^{4+} in the crystal lattice, the defects such as aluminium ions vacancies appeared. These defect structures can improved fracture surface energy of Ti^{4+}:sapphire, so the strength and toughness were further improved.

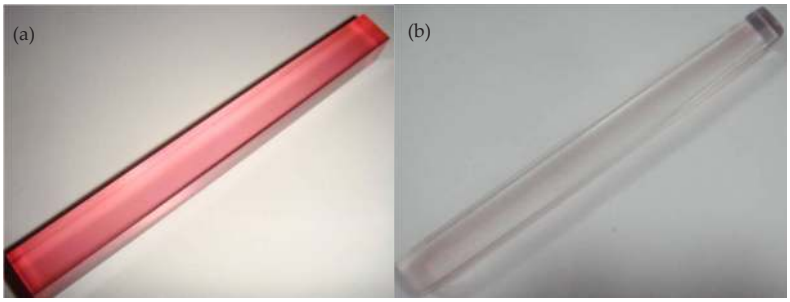

Figure 4. (a) Ti^{3+}:sapphire single crystal, (b) Ti^{4+}:sapphire (annealing 1600°C for 24h from Ti^{3+}:sapphire).

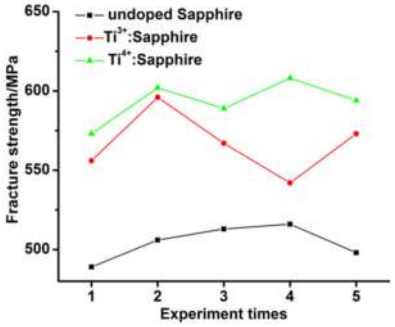

Figure 5. Fracture strength of Ti:sapphire and sapphire crystals.

3. Sapphire substrate crystal growth

3.1. Raw material

The raw materials (Al_2O_3) used for growing sapphire substrate crystal are divided into powder, sintered charge, cracked crystal and polycrystalline ingot, as is shown in Figure 6. In order to obtain LED grade sapphire crystal, Al_2O_3 raw material should be of high purity (≥99.996%) and high density. Table 4 presents the impurity concentrations of suitable Al_2O_3 analyzed by the inductively coupled plasmas optical emission spectroscopy (ICP-OES).

http://dx.doi.org/10.5772/54249

Cracked crystal stuff grown by Verneuil method without additives is commonly used. Due to undergoing a crystallization process, the purity and density of the cracked crystal raw material are much higher. Al_2O_3 polycrystalline ingot is prepared by the cold crucible induction skull melting technique (ISM) in recent years. The technical process is provided in Figure 7[13]. Al_2O_3 polycrystalline ingot could be made as a whole block according to the inside shape of the crucible used for crystal growth, which is convenient for charging.

The purities of sintered charge, cracked crystal and polycrystalline ingot are related to the purity of Al_2O_3 powder. Usually, the preparation methods of high purity Al_2O_3 powder include thermal decomposition of ammonium aluminum sulfate, thermal decomposition of ammonium aluminum carbonate hydroxide, aluminum isopropoxide hydrolysis method, aluminum choline hydrolysis method and high purity aluminum active hydrolysis method, etc[14,15]. The purity of the powder prepared by aluminum isopropoxide hydrolysis method is higher than that prepared by other methods. Impurities in raw material will reduce the transparency of crystal, make sapphire crystal pink or yellow, and increase dislocation defects that will cause LED luminous efficiency to decrease. Aluminum sulfate impurity from cracked crystal raw material decomposes again during crystal growth, which will make bubbles and insoluble remain in the sapphire. Excess Ca and Mg impurity ions will induce sapphire to crack, and excess K impurity ion will form scattering particles in the sapphire.

Figure 6. Al_2O_3 raw materials: (a) powder, (b) sintered charge, (c) cracked crystal, (d) polycrystalline ingot.

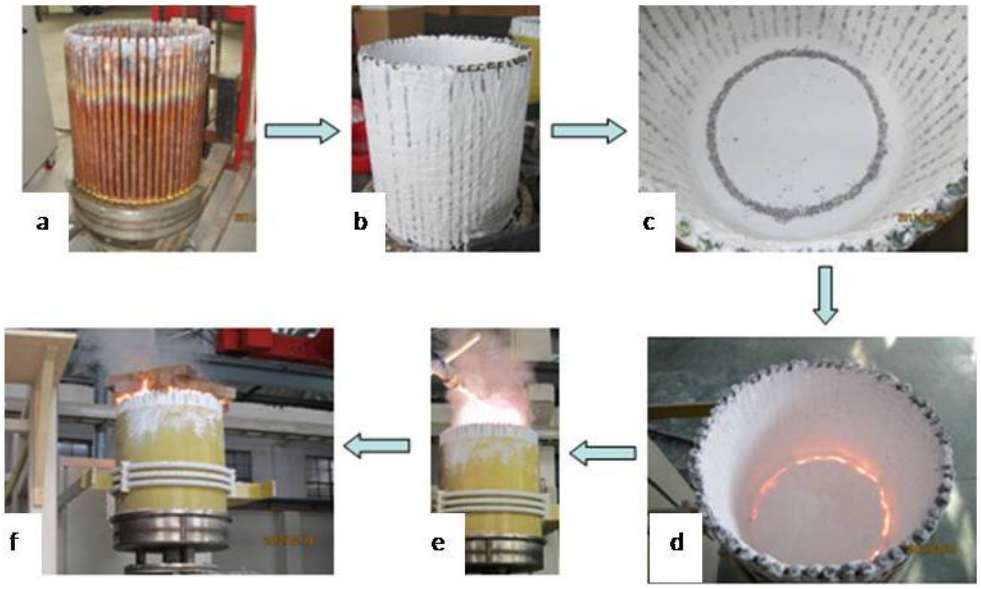

Figure 7. The process of Al_2O_3 polycrystalline ingot prepared by ISM.

Element	Na	Mg	Si	K	Ca	Ti	Cr
Concentration (μg/g)	<1	<1	<4	<1	<1	<1	<1
Element	Mn	Fe	Ni	Cu	Zn	Ga	Zr
Concentration (μg/g)	<1	<4	<1	<1	<1	<1	<1

Table 4. Impurity concentration analysis of suitable Al_2O_3 raw material.

3.2. Seed crystal

The selection of Al_2O_3 seed crystal is an important step before crystal growth. Sapphire crystal will inherit some defects in the seed crystal, and therefore seed crystal of high crystalline quality is absolutely necessary. The seed crystal should be colorless transparent, free from bubbles, inclusions, precipitations, twin crystal, grain boundary, microcrack and scattering particles.

3.3. Growth direction

The slip systems of sapphire reported so far are $(0001)1/3\langle 11\bar{2}0\rangle$ basal slip, $\{11\bar{2}0\}\langle 1\bar{1}00\rangle$ prism slip and $\{10\bar{1}1\}1/3\langle \bar{1}101\rangle$ pyramidal slip [16]. Slip is easy to occur along the direction of high atomic density. Among these systems, basal slip is the easiest slip system at high temperatures. When the obliquity between growth interface and (0001) plane is small, basal slip is prone to induce a large number of grain boundaries, even slip band and twin crystal.

http://dx.doi.org/10.5772/54249

On the contrary, it is not easy to slip and generate grain boundaries. Therefore, sapphire crystal is usually grown along a[11$\bar{2}$0], m[10$\bar{1}$0] or r[1$\bar{1}$02] direction to reduce sub-grain and twin boundaries defects.

3.4. Growth methods

3.4.1. Kyropoulos method

Kyropoulos (KY) method was put forward by Kyropoulos as early as 1926, and is used to prepare and study on large-size halogen group crystals, hydroxide crystals and carbonate crystals. Modified by Musatov in 1970's, Kyropoulos method is applied to grow sapphire single crystal. A schematic diagram of the KY furnace is shown in Figure 8. The crystal growth systems include vacuum system, heating system, cooling system, insulation system and control system. This method adopts the tungsten resistance-heated element, and the heat is transferred to the whole thermal field through radiation. Crystallization occurs when the seed contacts the melt at a temperature slightly lower than the melting temperature. The crystal gradually grows by water cooling from the seed holder and stably programmed reduction of the heat power to adjust the temperature distribution of the melt. The growth procedure is divided into seeding, shouldering, equal diameter growth, annealing and cooling. The crystals are usually boules, and the diameters could be 10~30 mm smaller than the crucible inner diameters. During the whole growth process, the crystal is in the crucible but no contact with the crucible wall, and located in the hot zone, thus the thermal stress in the crystal is small. At present, Kyropoulos method is one of the effective and mature methods to grow large diameter sapphire substrate crystals. In 2009, 200 Kg weight sapphire boule

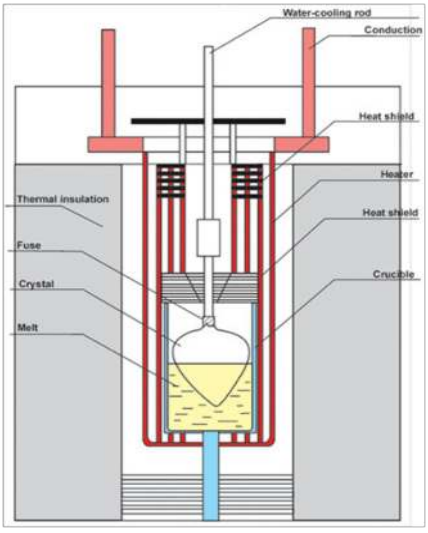

Figure 8. Schematic diagram of the resistance-heated KY furnace.

that is current world's largest sapphire crystal was successfully grown by Rubicon Technology Inc. using improved Kyropoulos method, proprietary ES2 crystal growth technology. Figure 9 shows the sapphire boule. Now, Rubicon has produced in mass 85 Kg grade sapphire boules, which is world leading level.

In China, the sapphire industry is developing rapidly. Many enterprises have built complete processes including sapphire growing, drilling, slicing and polishing which cover the entire industry chain. Under the leading of Prof. Xu, our team has developed advanced Kyropoulos method by optimizing furnace automatic closed-loop control system, thermal field system and growth technology. Melt convection, melt/crystal interface shape, temperature distribution and radiative heat exchange during the sapphire crystal growth process are analyzed systematically with CGSim software package of STR. Flow pattern in the melt at the melting temperature before modifications is displayed in Figure 10. The melt flow had a two-vortex structure: one is a larger vortex occupying the melt core, which is the normal melt convection; and the other is a smaller vortex of lower intensity located near the melt free surface, which is the abnormal melt convection. The melt flow direction of the smaller vortex is opposite to that of the main vortex. It is easy to cause overcooled melt to enrich in the area of the smaller vortex. The sapphire crystal will adhere to the crucible at the shouldering stage. The theoretical predictions are consistent with the experimental results. Isothermal changes at different growth stages and the small vortex gradually disappears at the cylindrical growth stage, which is demonstrated in Figure 11. After a series of modification in thermal field structure, the melt flow pattern of abnormal small vortex disappears completely, as is displayed in Figure 12. The thermal field is of reasonable temperature distribution, stable melt vortex, and has long service life and low cost. Our advanced Kyropoulos method has been successfully applied to the mass

Figure 9. Sapphire boule grown by Rubicon Technology Inc.[17].

http://dx.doi.org/10.5772/54249

production of 65K g grade sapphire boules and pilot production of 85 Kg grade sapphire boules in several domestic companies. Figure 13 shows the 65 Kg and 85 Kg grades sapphire boubles. The KY furnace is designed and developed by our team and Shenyang Scientific Instrument Co., Ltd., Chinese Academy of Sciences (SKY), and manufactured by SKY. The full width at half maximum of X-ray double crystal diffraction of 4″ sapphire wafer is less than 10 arc sec, and the average density of dislocations is about 1.99×10^{2} cm^{-2}.

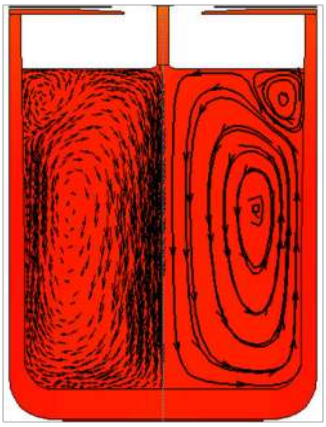

Figure 10. Flow pattern in the melt before modifications at the melting temperature.

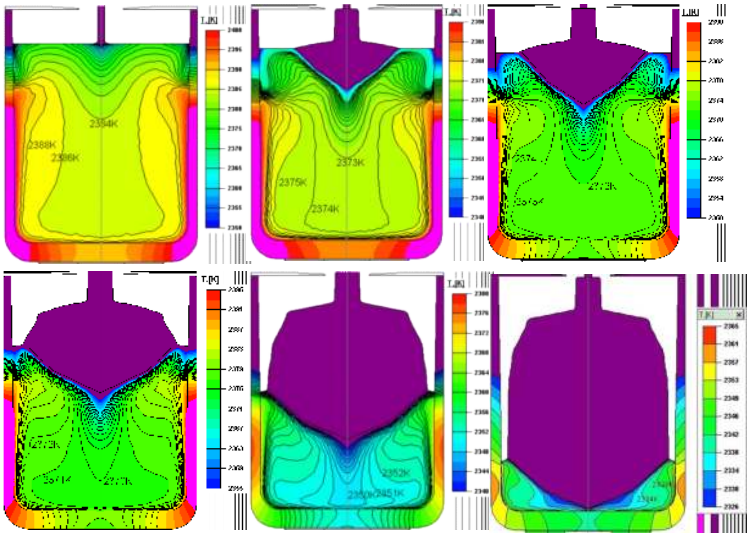

Figure 11. Isotherms at different growth stages.

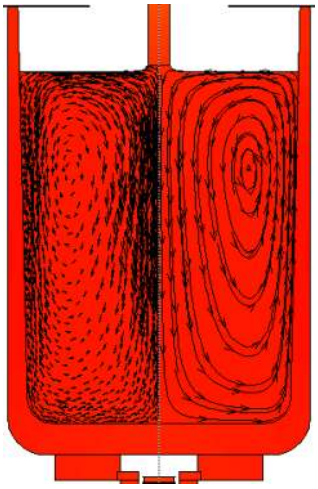

Figure 12. Flow pattern in the melt after modifications at the melting temperature.

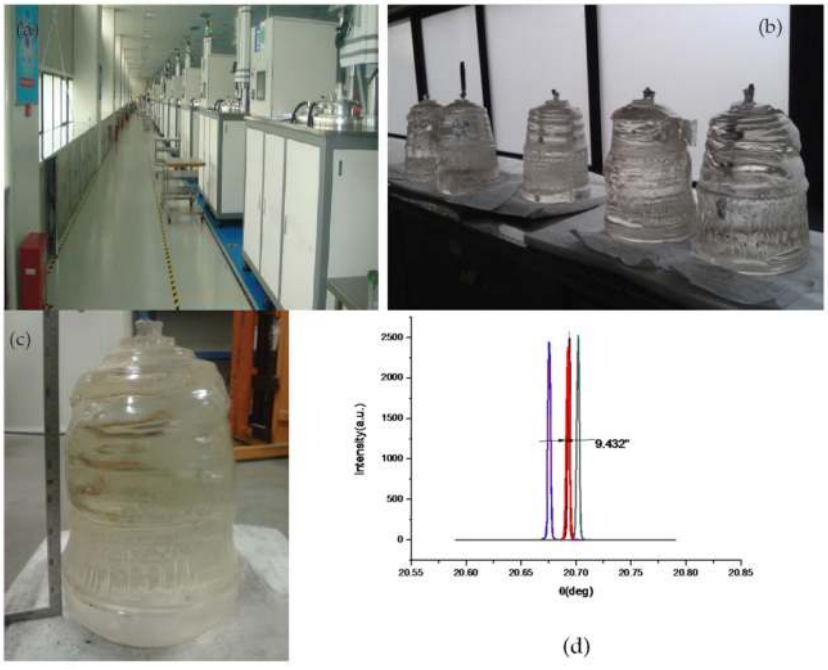

Figure 13. (a) KY furnaces manufactured by SKY, (b) 60 Kg, 85 Kg grades sapphire boules, (c) 83 Kg sapphire boule,(d) X-ray rocking curves of 4″ sapphire wafer in the center and at the edge.

http://dx.doi.org/10.5772/54249

3.4.2. Heat exchanger method

The heat exchanger method (HEM) for growing large sapphire crystal was invented by Fred Schmid and Dennis Viechnicki at the Army Materials Research Lab in Watertown, Massachusetts in 1967[18]. The modern implementation of Schmid and Viechnicki's heat-exchanger method at Crystal Systems in Salem, Massachusetts is depicted in Figure14. A high temperature heat exchanger is introduced from the bottom of the furnace into the heat zone. As the heat exchange medium, helium gas circulates in the heat exchanger to take out the heat. The control of the crystal growth process is achieved by adjusting the helium flow. After partial melting of the seed, gas flow is increased to initiate crystallization of melt onto the seed. When the crystallization is complete, the furnace temperature and the helium flow are decreased, and the boule is slowly annealed in situ. During the whole growth process, the crystal is surrounded by the high-temperature melt. It is difficult to release crystalline latent heat, so the growth rate of the crystal is constrained.

The application and development of HEM is mainly in the United States. GT-Solar and ARC Energy are two leading companies in this field. GT-Solar has grown 115 Kg sapphire crystal along a-direction. Heat is supplied by the graphite resistance heat; so that the crystal interior forms oxygen vacancies and the sapphire crystal is pink. Besides, the molybdenum crucible is disposable, thus the cost is high. Figure 15 shows the 111.40 Kg sapphire grown by Guizhou Haotian Optoelectronics Technology Co., Ltd. using the GT-Solar furnace. As we all know, growing high-quality sapphire crystals along c-direction is a great challenge. ARC Energy has achieved a certain degree of technological breakthroughs. They have grown 37 Kg and 47 Kg grades sapphire crystals along c-direction. Figure 16 shows the Φ170 mm and Φ260 mm sapphire ingots grown by ARC Energy. Compared with GT-Solar furnace, heat is supplied by the tungsten resistance-heated element on ARC Energy furnace, thus the sapphire crystal is colorless transparent. Due to sub-grain boundary defect, it is difficult to grow large size and high-quality sapphire crystal along c direction.

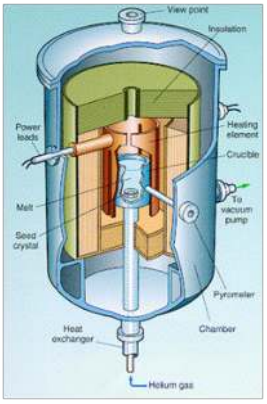

Figure 14. Schematic of a HEM furnace [19].

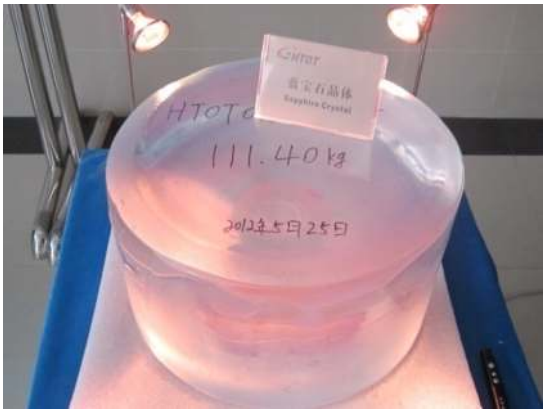

Figure 15. 111.40 Kg sapphire ingot.

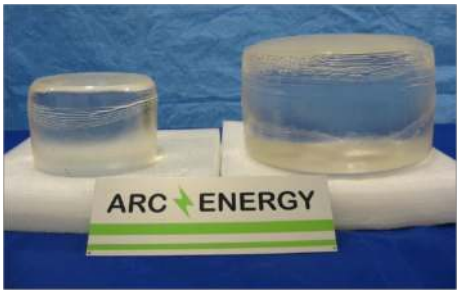

Figure 16. Sapphire ingots (Φ170 mm & 260 mm) grown by ARC Energy.

3.4.3. Czochralski method

The Czochralski method is named after Jan Czochralski who introduced an early version in 1916, and published it as a method for studying the crystallization rate of metals [20]. Further modifications by Teal and Little brought the technique closer to the process known as the Czochralski or CZ method [21]. This technique was first applied to grow sapphire crystal by Poladino and Rotter in 1964, and the quality of the as-grown sapphire crystal was relatively high. Figure 17 presents the Czochralski furnace geometry. The crucible is heated by means of an rf generator operating in the range of 10-30 kHz. Considering the melting point of sapphire is 2050°C, Ir crucible whose highest working temperature is up to 2200°C is commonly used. The growth and control of the sapphire crystal is dependent upon the automatic diameter control system that weighs the crystal while it is growing. The change in crystal weight is used to generate a control signal that modifies the generator output power

http://dx.doi.org/10.5772/54249

to the crucible, thereby controlling the diameter is achieved through small changes in the liquid temperature. The crystal is constantly rotated and pulled during the growth process, which is different from Kyropoulos method. The main advantages of CZ method are automatic diameter control, convenient to observe the growth status of crystal. Through technique improvement, UNC Co.Ltd. has grown 4″ and 6″ sapphire crystals along a or c direction by CZ method.

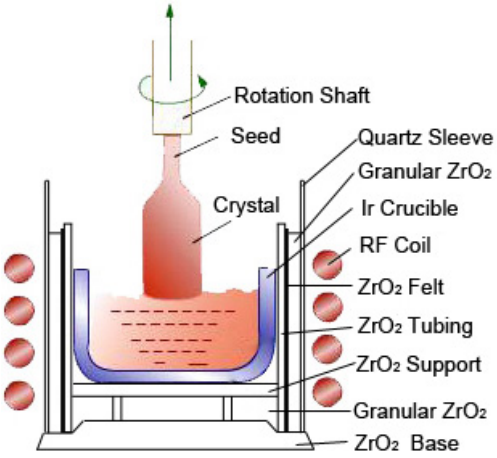

Figure 17. Schematic of a typical Czochralski furnace.

3.4.4. Edge-defined film-fed growth method

Edge-defined film-fed growth method was invented by Harold Labelle and Stepanov in 1960's [23]. This technique is used to grow special-shaped crystals, such as ribbon, tubal and nemaline crystals. Figure 18 shows the schematic diagram of the EFG furnace. The mold with capillary slit is put in the melt. The melt rises to the top of the mold due to the capillarity, forming a layer of thin film and spreading to the surrounding, at the same time crystallization starts from the seed. Melt rising height H is calculated by $H=2\gamma\cos\theta/(\varrho dg)$, where γ denotes the melt surface tension coefficient (N/cm), ϱ denotes the melt density (g/cm^3), d denotes the capillary diameter (cm), g denotes acceleration of gravity (N/g) and θ denotes solid-liquid wetting angle ($0°<\theta<90°$). The wetting angle of melt and mold should be less than 90° so as to form melt fluid film of a certain thickness. The advantages of EFG are that growth rate is fast, the cost is low, and multiple-piece crystals can be grown simultaneously. Figure 19 exhibits the substrate-grade sapphire ribbons grown by Namiki company whose technique is advanced in the world. The magnitude of dislocation density is about $10^{3\text{-}5}$cm^{-2} which is two magnitudes lower than that of grown by conventional EFG method. The main defects of sapphire crystal grown by EFG are bubble, grain boundary, dislocation and heat stress, resulting from overcooling temperature at the solid-liquid interface.

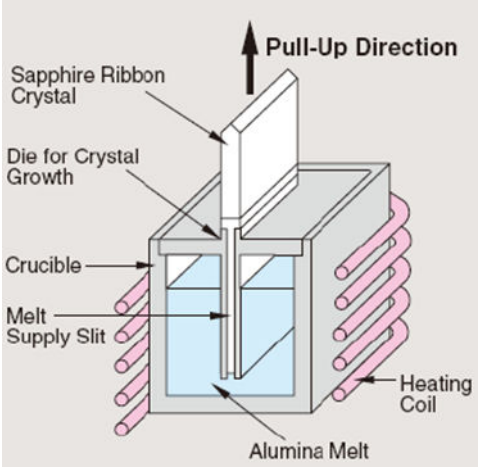

Figure 18. Schematic diagram of sapphire crystal grown by the edge-defined film-fed growth method[23].

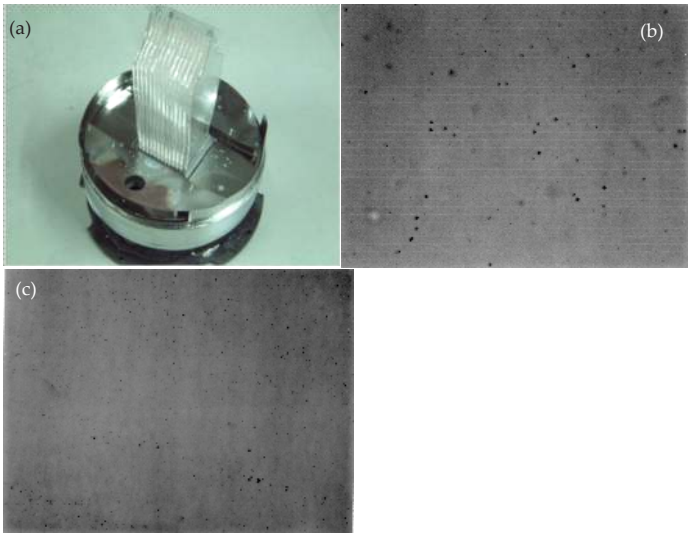

Figure 19. (a) Sapphire ribbons grown by Namiki company, (b) Dislocation density of sapphire wafers grown by conventional EFG, (c) Dislocation density of sapphire wafers grown by Namiki.

3.4.5. Temperature gradient technique

The temperature gradient technique (TGT) is a typical static directional solidification technique, invented by Cui et al. from Shanghai Institute of Optics and Fine Mechanics(SIOM) in

http://dx.doi.org/10.5772/54249

1979[22]. A schematic diagram of the TGT furnace is shown in Figure 20. It consists of molybdenum crucible, graphite heating element and molybdenum heat shields. The cylindrical graphite heat element is designed as an electric circuit with proper linear resistance from the top to the middle by making holes in certain distribution. The cylinder is placed in the graphite water cooled electrodes. The temperature gradient of the upper part is built by the linear resistance of the heating element, and that of the lower depends on the extraction of heat by water flowing in the tubes through the electrodes. Besides, the temperature field near the seed is influenced by the heat conductivity of the water-cooled centre rod. The temperature gradient is in the opposite direction of gravity, and there are no moving parts in TGT. The growth process is accomplished by dropping temperature at designed rates with a high precision temperature program controller.

Figure 21 shows the sapphire crystals grown by TGT. The graphite volatilizes to a certain extent, which makes the atmosphere oxygen-lacked. In the reducing atmosphere, transition metal impurity ions exist in the low valence form (e.g.: Cr^{3+}, Ti^{3+}), so that sapphire crystals are pink or light green. In order to improve optical transmittance and uniformity, the sapphire crystals must undergo annealing treatment of decarbonisation and decolorisation. The annealing treanment has two steps. At first, the sapphire crystals are annealed in oxidizing atmosphere at 1700°C, and then annealed in strong reducing atmosphere at 1600-2200°C. After the special annealing process, the color can be eliminated and sapphire crystals revert to high optical property.

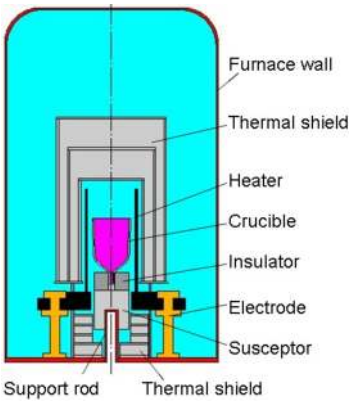

Figure 20. Schematic diagram of a TGT furnace.

3.5. Crystal defects

With the fast development of modern science and technology, the requirements of sapphire materials are getting higher and higher. A popular standard of sapphire substrate wafer for GaN epitaxy is as follows [24]: purity >99.999%, orientation accuracy <±0.5°, dislocation density $<1\times10^{3}$ cm^{-2}, carbon content $<5\times10^{9}$ cm^{-2}, number of particles bigger than

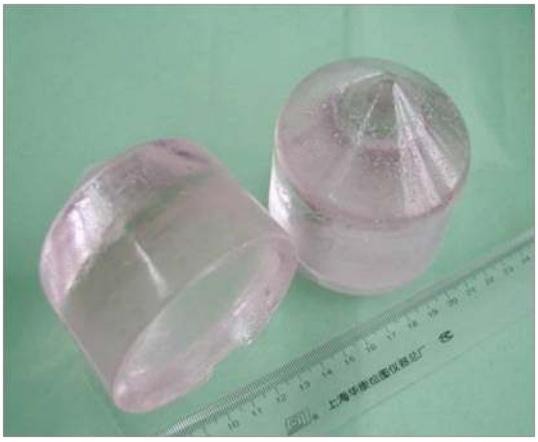

Figure 21. Sapphire crystals grown by TGT.

0.1μm <20/piece. Sapphire crystals grown from the melt usually contain various types of macro or micro defects, among which dislocations, sub-grain boundaries, inclusions, crack, bubbles are common. The distribution of each kind of defects in sapphire depends on each process of the production, from raw material preparation to crystal growth and subsequent heat treatment. Studying the origin and the distribution behavior of defects can deliver a better understanding on crystal growth process, which may provide solid information to production improvement.

3.5.1. Dislocations

Dislocation is one of the common microscopic defects in the sapphire crystals. Figure 22 shows the dislocation corrosion morphology of sapphire wafer grown by TGT [25]. In TGT, the crystal touches crucible, which can cause a stress field, especially during cooling process. Such stress field can cause plastic deformation of the crystal by activating the slip systems. And more dislocations are formed. The typical etch pits generated on (0001) plane are triangles, and on $(11\bar{2}0)$ plane are rhombuses. The dislocation corrosion morphology is determined by the point group and structure of the crystal. The role of the chemical etchant is to destroy the bonds between molecules or atoms inside the crystal, and the smaller bond strength is first to be destroyed, thus forming a particular shape of the corrosion spots. Figure 23 reveals that the density of etch pits on the different position of the sapphire crystals is not uniform. It is higher at the shoulder and lower at the equal-diameter position of the crystals.

The origins of the dislocations in the sapphire crystals are as follows: (1) dislocations inheriting from the seed, including the seed dislocations and the dislocations introduced during seed machining process and seeding process; (2) dislocation nucleation and multiplication produced when the thermal stress in the crystal exceeds the critical stress; (3) external thermal and mechanical fluctuation.

http://dx.doi.org/10.5772/54249

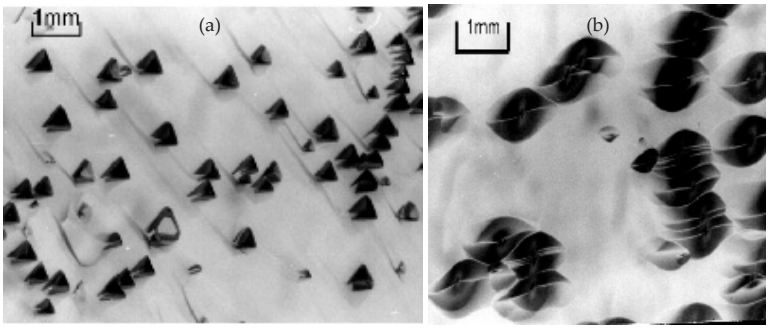

Figure 22. Dislocation corrosion morphology of sapphire wafers: (a) (0001) plane, (b) $(11\dot{2}0)$ plane.

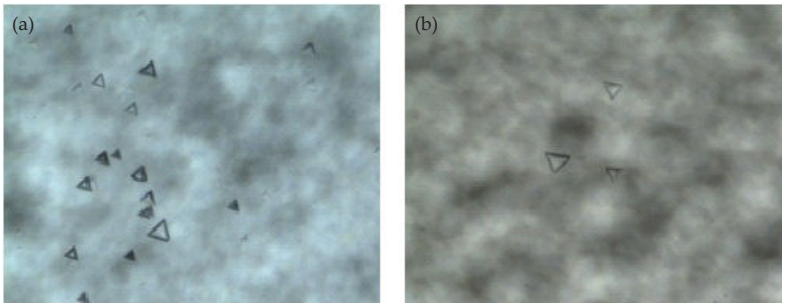

Figure 23. Dislocation etch pits on the (0001) plane of sapphire wafers grown by KY method:(a) shoulder position, (b) equal diameter position.

3.5.2. Sub-grain boundaries

Mosaic structure is the fine structural regions of the crystallographic misorientation smaller than 10°C. The boundaries between the two regions are known as sub-grain boundaries. Figure 24 shows the mosaic structure on (0001) plane of the sapphire blocks under the polariscope. The area of the mosaic structure has colored interference fringe, which is different in color from the main part of the crystal. Sub-grain boundaries could also be observed by chemical etching method, as is shown in Figure 25.

Dislocation sub-grain boundaries are usually formed on cooling or annealing procedures. During these periods, the dislocations acquire sufficient excitation energy to migrate. Then under the stress-field interaction, the dislocations on the different slip planes stop at equilibrium positions, and form the sub-grain boundaries. In addition, the lineage structure appearing in the melt crystallization process can also lead to the formation of sub-grain boundaries [26]. Therefore, the basic method to eliminate sub-grain boundaries is to reduce

the dislocation density and thermal stress in the sapphire crystals. Meanwhile, the growth direction should be a[11$\bar{2}$0], m[10$\bar{1}$0] or r[1$\bar{1}$02] direction, not c [0001] direction as possible.

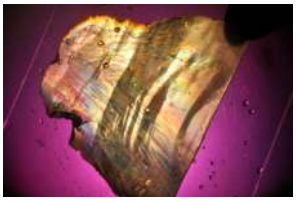

Figure 24. Optical image of the mosaic structure on (0001) plane of the sapphire blocks.

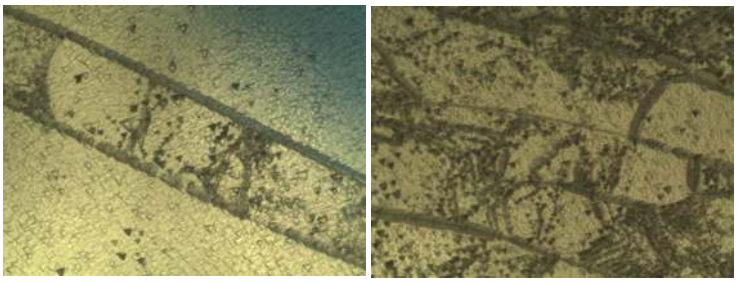

Figure 25. Optical image of sub-grain boundary obtained after the (0001) plane slice has been etched in KOH melt at 380℃ for 10 min.

3.5.3. Inclusions

Inclusion is a common macroscopic defect in the sapphire crystal grown by melt method. The impurity elements of Al_2O_3 raw material and crucible material, as well as tungsten, molybdenum fragments from the crucible, heating unit and insulations will form inclusions in the crystals. Due to the impurity discharging phenomenon, impurities in the raw materials discharge to the edge, and impurities in the crucible diffuse to the centre. These impurities precipitate when the concentration exceeds the saturated concentration in the melt, forming inclusions. Therefore, high purity of Al_2O_3 raw material, crucible material and insulation material are important to grow high quality sapphire crystal.

3.5.4. Cracking

Cracking is one of the main defects of large size sapphire crystal. It is divided into stress cracking and polycrystalline cracking, as is shown in Figure 26. The crystal with stress is also easy to crack along cleavage plane during drilling rod process. Figure 27 reveals the cracked sapphire rod. In addition, because the crystal and crucible material are different in

http://dx.doi.org/10.5772/54249

the thermal expansion coefficients, the sapphire crystal is prone to crack on the annealing or cooling procedure if the crystal touches the crucible.

The crystal growth process is mainly achieved by controlling the heat transport system, thus the crystal itself is bound in a certain temperature gradient in the thermal field. When the crystal growth rate or cooling rate is too fast, too large temperature gradient is bound to lead to large thermal stress inside the crystal. Stress in the crystal causes the strain. The cracks initiate, expand and the crystal will crack when the strain exceeds the yield limit. Figure 28(a) presents the interference photographs of the (0001) plane sapphire crystals with stress. The colored strip is asymmetric, and the dark line of the extinction figure shows distortion.

Figure 26. Cracking in large size sapphire crystals: (a) stress cracking, (b) polycrystalline cracking.

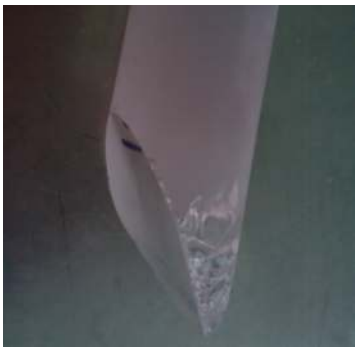

Figure 27. Cracking in the sapphire rod with stress.

3.5.5. Bubbles

Figure 29 presents the bubble distribution of the sapphire boule examined by He-Ne laser. The bubble content is higher at the shoulder and center of the crystal, and the quantity and size of the bubble decrease on the equal diameter position. When the crystallization rate is

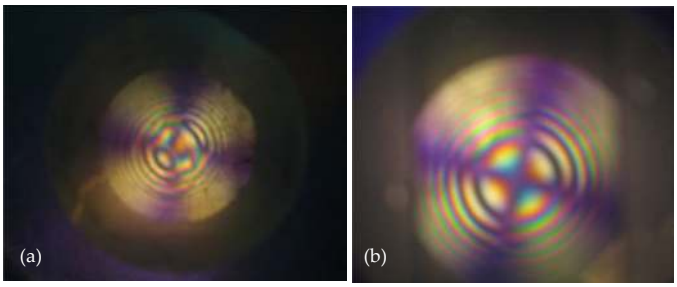

Figure 28. Interference photograph of (0001) plane sapphire rods under the polarizing microscopy:(a) sapphire bar with stress, (b) sapphire bar without stress.

too fast, the bubbles in the melt cannot be removed thoroughly, and bubble layer will form in the crystal. That the separation coefficients of the gas in the solid and melt are different is the reason for the formation of bubbles.

Mycatob et. al thought that micro-thermal decomposition of the alumina melt release O_2, and tungsten, molybdenum and oxygen react chemically. The chemical reaction equations are as follows [27]:

$$\mathrm{Mo(s)} + \tfrac{3}{2}\mathrm{O_2(g)} \rightarrow \mathrm{MoO_3(g)}$$

$$\mathrm{Wo(s)} + \tfrac{3}{2}\mathrm{O_2(g)} \rightarrow \mathrm{WO_3(g)}$$

When the crystalline rate is too fast or the fluctuation of crystal growth rate is too large, the gas can be easily captured and wrapped from the solid-liquid interface into the crystal.

Bunoiu et. al have put forward a model to explain the origin and distribution of bubbles in EFG sapphire. According to this model, the origin of the bubble formation is attributed to the reactions described as follows:

$$\mathrm{Al_2O_3}(l) \rightarrow \mathrm{2O(g) + Al_2O(g)}$$

$$\mathrm{Mo(s) + Al_2O_3}(l) \rightarrow \mathrm{MoO(g) + Al_2O(g) + O(g)}$$

$$\mathrm{Mo(s) + O(g) \rightarrow MoO(g)}$$

$$\mathrm{Mo(s) + Al_2O(g) \rightarrow MoO(g) + 2Al(g)}$$

$$\mathrm{O(g) + C(s) \rightarrow CO(g)}$$

$$\mathrm{Al_2O(g) + C(s) \rightarrow CO(g) + 2Al(g)}$$

$$\mathrm{3MoO(g) + 5C(s) \rightarrow Mo_3C_2(g) + CO(g)}$$

The main composition of the bubble is CO, which has been verified through spectroscopy. They also used numerical simulation to explain the distribution of bubbles and also devel-

oped a way to confine bubble distribution near the surface, so it can be easily removed through polishing [28].

Figure 29. The bubble distribution of the sapphire boule grown by KY method.

4. Conclusions

The growth methods of sapphire nearly cover all of the crystal growth technology, and each method has its own uniqueness. However, Kyropoulos method, edge-defined film-fed growth method, heat exchanger method are the main methods used in mass production in the world, and Kyropoulos method and heat exchanger method are more universal. Table 5 lists the advantages and disadvantages of sapphire crystal growth methods. CZ method is mainly used to grow 3″ sapphire crystals, and HEM, TGT and KY methods are mainly used to grow larger than 4″ sapphire crystals. As the requirements of sapphire substrate constantly improve, the techniques to grow larger sapphire crystal are under research.

Method	Advantages	Disadvantages
KY	High quality and large-size crystal Fast growth rate	Low automation degree High technical requirement on operator
HEM	High automation degree Large size crystal	High cost
CZ	High automation degree	High cost Small size crystal
EFG	Fast growth rate Low cost	The orientation adjustment of large size crystal is difficult.

Table 5. The characteristics of sapphire substrate growth methods from the industrial point of view.

Author details

Huili Tang, Hongjun Li and Jun Xu

*Address all correspondence to: xujun@mail.shcnc.ac.cn

Shanghai Institute of Ceramics, Chinese Academy of Sciences, Shanghai, China

References

[1] Huili Tang. Study of growth and characterization on $ScAlMgO_4$, $Mg_{0.4}Al_{2.4}O_4$ novel substrate crystals. PhD thesis. Shanghai Institute of Ceramics, Chinese Academy of Sciences;2010.

[2] Elena R. Dobrovinskaya, Leonid A. Lytvynov, Valerian Pishchik, Sapphire Material, Manufacturing, Applications. 2009,P 55-56.

[3] Kecong Zhang, Lehui Zhang. Crystal Growth (version l).1981. P464-465.

[4] Conglu Wang. Sapphire single crystal (version l). 1982.P4-6.

[5] Ni X, Özgür Ü, Baski A. A., Morkoç H., Zhou Lin, David J. Smith and Tran C. A..Epitaxial Lateral Overgrowth of Semipolar GaN on (11−00) m-plane Sapphire by Metal-organic Chemical Vapor Deposition. Appl. Phys. Lett.90 2007; 182109.

[6] P. Vennéguès and Z. Bougrioua. Epitaxial orientation of III-nitrides grown on R-plane sapphire by metal-organic-vapor-phase epitaxy. Appl. Phys. Lett. 2006; 89, 111915.

[7] B. A. Haskell, F. Wu, S. Matsuda, M. D. Craven, P. T. Fini, S. P. DenBaars, J. S. Speck and Shuji Nakamura. Structural and Morphological Characteristics of Planar (112¯0) a-plane Gallium Nitride Grown by Hydride Vapor Phase Epitaxy. Appl. Phys. Lett. 2003;83(8), 1554-1556.

[8] T. Paskova, R. Kroeger, S. Figurege, D. Hommel, V. Darakchieva, B. Monemar, E. Preble, A. Hanser, N. M. Williams, and M. Tutor. High-quality Bulk a-plane GaN Sliced from Boules in Comparison to Heteroepitaxially Grown Thick Films on r-plane apSphire. Appl. Phys. Lett. 2006;89, 051914.

[9] X. Nia, Y. Fu, Y.T. Moon, N. Biyikli, H. Morkoc. Optimization of (112¯0) a-plane GaN Growth by MOCVD on (112¯0) r-plane Sapphire. J. Cryst. Growth 2006; 290 166-170.

[10] Chun-Hung Chen, Jyh-ChenChen, Chung-WeiLu, Che-MingLiu. Numerical Simulation of Heat and Fluid Flows for Sapphire Single Crystal Growth by the Kyropoulos Method. J. Cryst. Growth 2011; 318 162-167.

[11] Hosseini S M, Aliabad H A R, Kompany A.. First-principles Study of the Optical Properties of Pure α-Al_2O_3 and La aluminates. Eur Phys J B 2005; 43(4): 439-444.

[12] http://www.mkt-intl.com/index.shtml.

[13] Jiao Wang. Synthesis of Polycrystalline α-Al2O3 Prepared by Cold Crucible Method and Study of Defects on Sapphire crystal by Kyropous. Master. Zhengzhou University;2012.

[14] Gaofeng Fu, Shiwen Bi, Xudong Sun, Yihong Yang. The Preparation Technique of Ultrafine Alumina Powders. Non-ferrous Mining and Metallurgy. 2000; 16(1), 39-41.

[15] Jianliang Liu, Jialin Sun, An Shi, Jin Hu, Xianyong Lu, Fuqian Zheng. Recent Development of the Methods to Make the High Purity Fine Alumina. Joumal of Kunming University of Science and Technology(Science and Technology). 2003; 28(3),22-24.

[16] Atsutomo Nakamura, Takahisa Yamamoto and Yuichi Ikuhara. Direct Observation of Basal Dislocation in Sapphire by HRTEM, Acta Materialia 2002;50 101-108.

[17] http://tech.oecr.com/.

[18] F. Schmid and D. Viechnicki. Growth of Sapphire Disks from the Melt by a Gradient Furnace Technique. J. Am. Ceram. Soc. 1970;53 528.

[19] D. C. Harris. A peek into the history of sapphire crystal growth,.Proc. SPIE 2003;5078 1-11.

[20] J. Czochralski. A new method for the measurement of crystallization rate of metals. Zeitschrift des Vereines Deutscher Ingenieure 1917;61 245-351.

[21] G. K. Teal and J. B. Little. Growth of germanium crystals. Phys. Rev. 1950;78 647.

[22] F. Cui, Y. Zhou, J. Qiao. Growth of high quality monocrystal sapphire by seed-induced Temperature Gradient Technique (STGT). J. Chin. Ceram. Soc. 1980;8 109-113.

[23] Bunoiu O M, Nicoara I, Santailler J L, et al. On the void distribution and size in shaped sapphire crystals. Cryst Res Technol,2005;40(9) 852-859.

[24] Hai Zhou, Shaofeng Yao. Study of the system of quality inspection for sapphire wafer. Applied Science and Technology 2005;32(11):21-24.

[25] Guoqing zhou. Study of Defects and Growths on Sapphire and α-BaB_2O_4 Crystals, PhD thesis. Shanghai Institute of Optics and Fine Mechanics, Chinese Academy of Sciences;1997.

[26] HongJun Li, GugJuann Zhao, XiongHui Zeng, ZhenYing Qian, JuPing Guo, ShengMing Zhou, Jun Xu. Low-angle Boundary in High-temperature Scintillating Crystal Ce:YAP. Journal of Inorganic Materials 2004; 19(5):1186-1190.

[27] М.И. Мусатов. Причины образования пузырей в кристаллах корунда. Неорганические материалы. 1979; 15(10):1806-1810.

[28] Bunoiu, O.M., T. Duffar, and I. Nicoara. Gas bubbles in shaped sapphire. Progress in Crystal Growth and Characterization of Materials 2010; 56(3–4) 123-145.